05

Resonant dynamics of the magnetization of uniaxial nanoparticle

© A.M. Shytyi, T.M. Vasilevskaya, D.I. Sementsov¶

Ulyanovsk State University,
Ulyanovsk, Russia

¶ E-mail: sementsovdi42@mail.ru

Received February 21, 2022
Revised February 26, 2022
Accepted February 27, 2022

Analysis of equilibrium conditions was carried out and resonant precessional dynamics of magnetization of a single-domain magnetically uniaxial ellipsoidal particle. Considered the case when magnetic field is along the easy magnetization axis. the easy magnetization axis is directed parallel to the axis of symmetry of the ellipsoid and transverse to pumping by a weak high-frequency field. Features of the behavior of the magnetization were discovered. It has been revealed that the magnetization has features of resonant behavior: large resonant precession angles with amplitude $0.5M_0$, elliptical deviations of the precession trajectory from circular at a negative value of the effective anisotropy field, and the presence of a frequency region with nonlinear precession for an oblate nanoparticle.

Keywords: ferromagnetic resonance, elliptical nanoparticles, transverse bias field, effective anisotropy, bistability, easy magnetization axis, nonlinear effects.

DOI: 10.21883/PSS.2022.06.53825.279

1. Introduction

It is known that recording of data on lattice structures of magnetic nanoparticles (NP) is based on changing an equilibrium configuration of magnetic moments of individual nanoparticles due to impact of a local magnetic field pulse. In doing so, data reading can be implemented by exciting the configuration occurred by a weak radio pulse at a frequency of ferromagnetic resonance (FMR) [1–5]. In connection therewith, significant interest is paid to understanding fundamental behavior of a spin subsystem in an external static and high-frequency magnetic field in the nanoparticle, with the complex configuration of internal fields including exchange, dipole-dipole and magnetostatic fields, a crystalline anisotropy field. At this, many FMR features are defined by geometric factors — a size of the nanoelements, a shape and a ratio of their sides, spatial arrangement in the structure [6–9]. Thus, many studies in this field are focused on studies of FMR in thin-film elliptical and rectangular microstrips of a nanometer thickness, which are regarded as one of the main geometric elements for data recording and processing. At this, besides a main „homogeneous“ FMR mode, the experiment also showed an evident resonance peak depending on the thickness, which is correlated to heterogeneity of the internal field and, therefore, of distribution of the magnetization at angles and edges of the microstrips [10,11].

In order to interpret results to be obtained therein, it is also necessary to take into account that a position of the FMR line and its form substantially depend not only on the configuration of the structure itself, but on the size and symmetry, a magnetization equilibrium state, a type and value of magnetic anisotropy of individual nanoparticles. At the same time, the heterogeneity of the internal magnetostatic field near microstrip boundaries leads to localized edge modes in the resonance spectrum [12–17].

Special properties of 3D single-domain nanoparticles affecting their dynamic characteristics may also include bistability due to equilibrium orientation states with unequal projections of the magnetic moment, which are mutually translatable in controllable transitions with different precession modes during remagnetization [18–20]. In order to understand the impact of the bistability on FMR, a remagnetization type and dynamics of the magnetic moment in the lattice structure, it is necessary to take into account the above-mentioned factors in a mathematical model describing the said phenomena in an individual nanoparticle.

Based on analysis of the equilibrium conditions, the present paper gets equilibrium states for a single-domain magnetically uniaxial ellipsoidal nanoparticle when an „easy“ axis and a bias field are oriented along the axis of symmetry and various values of a form factor n (nonsphericity). Numerical solution of the Landau–Lifshitz equation for a region of collinear direction of magnetization and the external static field is based on to study features of the resonance dynamics when the weak transversal high-frequency field is switched on. Even for a slightly oblate nanoparticle at specified material parameters, a frequency range has been revealed to implement the dynamic bistability and observe FMR nonlinearity and a nutation type of the resonance precession.

2. General relationships

Let us consider a sample shaped as an ellipsoid of revolution. We assume that, besides the shape anisotropy, the sample has uniaxial anisotropy, which easy axis is coincident with the symmetry axis of the sample. In this case the free-energy density contains Zeeman energy, anisotropy energy, and energy of scattering fields [21,22]:

$$F = -\mathbf{M}(\mathbf{H}+\mathbf{h}) - \frac{K_u}{M^2}(\mathbf{Mn})^2 + \frac{1}{2}\mathbf{M}\hat{N}\mathbf{M}. \qquad (1)$$

Here $\mathbf{M}$ — NP magnetization, $\mathbf{H}$ and $\mathbf{h}$ — a static and high-frequency field, K_u — a uniaxial anisotropy constant, $\mathbf{n}$ — an anisotropy axis unit vector, $\hat{N}$ — a diagonal tensor of demagnetization factors, whose components are correlated in a relationship $N_x + N_y + N_z = 4\pi$ and depend on the form factor — a longitudinal-to-transversal semiaxis ratio of the ellipsoid $n = l_{\|}/l_{\perp}$. It is convenient to introduce the following parameters for the ellipsoid of revolution $N_{\perp} = N_x = N_y$, $N_{\|} = N_z$ and $\Delta N = N_{\perp} - N_{\|}$. Then, for an oblong and oblate ellipsoid ΔN is determined by the expressions:

$$\frac{\Delta N}{2\pi} = 1 - \frac{3}{n^2-1}\left[\frac{n}{\sqrt{n^2-1}}\ln\left(n+\sqrt{n^2-1}\right) - 1\right] > 0,$$

$$n > 1,$$

$$\frac{\Delta N}{2\pi} = 1 - \frac{3}{n^2-1}\left[\frac{n}{\sqrt{n^2-1}}\arcsin\sqrt{n^2-1} - 1\right] < 0,$$

$$n < 1, \qquad (2)$$

Taking into account the orientation of the „easy“ axis of the magnetic anisotropy along the symmetry axis of the ellipsoidal sample, it is convenient to introduce for consideration a field of effective anisotropy $H_{\mathrm{KN}} = 2K_u/M_0 + M_0\Delta N$, which will define its resonance behavior (here M_0 — saturation magnetization).

The Fig. 1 shows the dependence of the magnitudes H_{KN} and ΔN on the form factor n, obtained for the material parameters of the nanoparticle $K_u = 10^5\,\mathrm{erg/cm^3}$ and $M_0 = 800\,\mathrm{Gs}$. The magnitude axis is dotted with three values (0.95, 1.0, 1.05) corresponding to an oblate, spherical and oblong NP shape, which will be included in the below-shown numerical analysis of resonance behavior features. It is clear that depending on n the effective anisotropy field has regions of both negative and positive values. In the case under consideration, when n; 0.94 the field $H_{\mathrm{KN}} \simeq 0$ and when n is changing around this value, the field sign H_{KN} is reversed.

Time dependence of vector orientation $\mathbf{M}$ and, therefore, the NP magnetization's precession dynamics for various cases of bias and high-frequency pumping is determined on the basis of numerical solution of the Landau–Lifshitz equation [21,22]:

$$\frac{\partial \mathbf{M}}{\partial t} = -\gamma\,\mathbf{M}\times\mathbf{H}^{\mathrm{eff}} + \frac{\alpha}{M}\mathbf{M}\times\frac{\partial \mathbf{M}}{\partial t}, \qquad (3)$$

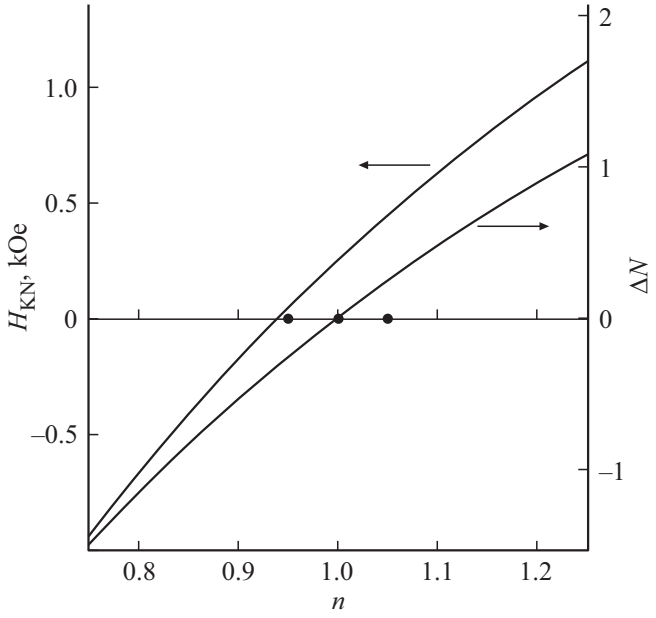

Figure 1. Dependence of the effective anisotropy field and the parameter ΔN on the semiaxis ratio of the ellipsoidal nanoparticle.

where $\gamma = 1.76\cdot 10^7\,(\mathrm{Oe}\cdot\mathrm{s})^{-1}$ — a magnetic & mechanic ratio, α — a dimensionless constant of attenuation, the effective magnetic field

$$\mathbf{H}^{\mathrm{eff}} = -\partial F/\partial \mathbf{M} = \mathbf{H} + \mathbf{h} + \frac{2K_u}{M_0}\mathbf{n} + \hat{N}\mathbf{M}. \qquad (4)$$

The equilibrium values of the polar θ_0 and azimuthal φ_0 angle, defining a direction of the vector $\mathbf{M}$ with reference to the ellipsoid symmetry axis (axis OZ) and the perpendicular axis (for example, OX), are to be found from the condition $\partial F/\partial\varphi = \partial F/\partial\theta = 0$. There is no dependence on the azimuthal angle in the basal plane under bias of the ellipsoidal nanoparticle along the symmetry axis ($\mathbf{H} \parallel \mathbf{n} \parallel OZ$) and the equilibrium angle φ_0 may be considered zero. For the oblong and spherical nanoparticle (when $n \geq 1$), the equilibrium polar angle θ_0 is zero at any field H. However, $\theta_0 = 0$ remains for the oblate nanoparticle ($n < 1$) as well up to the value $\Delta N = -(H + H_u)/M_0$. With further decrease in n the angle θ_0 changes in accordance with the expression:

$$\cos\theta_0 = -\frac{H}{H_u + \Delta N M_0}. \qquad (5)$$

The Fig. 2 shows the dependences of the longitudinal component of the magnetization $M_z = M_0\cos\theta_0$ on the form factor n, as obtained for values of the external field $H = 50$, $150\,\mathrm{Oe}$ (the curves *1, 2*). It is clear that the equilibrium vector remains parallel to the external field and the NP symmetry axis for $H = 50\,\mathrm{Oe}$ at $n > 0.928$, and for $H = 150\,\mathrm{Oe}$ at $n > 0.906$.

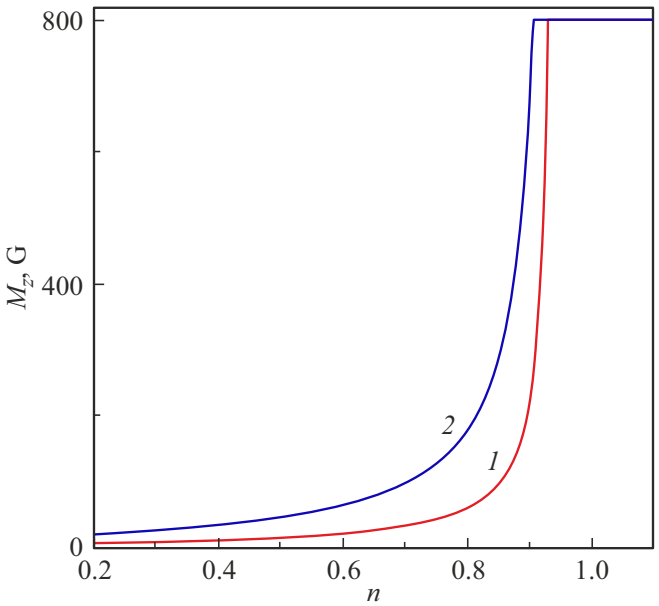

Figure 2. Dependences of the longitudinal component of the high-frequency magnetization on the form factor n, $H = 50,\ 150$ Oe (the curves *1, 2*).

In general, the frequency of the magnetization resonance precession is defined by the following expression:

$$\omega_{\text{res}} = \frac{\gamma}{M_0 \sin\theta_0}\left[\left(\frac{\partial^2 F}{\partial\varphi^2}\right)_0\left(\frac{\partial^2 F}{\partial\theta^2}\right)_0 - \left(\frac{\partial^2 F}{\partial\varphi\partial\theta}\right)_0^2\right]^{1/2}, \tag{6}$$

where second order derivatives of the free energy are calculated for the equilibrium angles φ_0 and θ_0. Under NP bias along the easy axis and the symmetry axis ($\mathbf{H} \parallel \mathbf{n}$) within the values n, where the equilibrium angle θ_0 is zero, taking into account (1) and (6), the dependence of the resonance frequency on the external field is determined by the following expression:

$$\omega_{\text{res}} = \gamma\left(H + \frac{2K_u}{M_0} + M_0\Delta N\right). \tag{7}$$

Note that quite small NP nonsphericity deviation substantially affects the value ΔN and, therefore, the field H_{KN}, thereby changing a position of typical values of the frequency $\omega_{\text{res}}(0)$ and the resonance dependences as a whole. As will be shown below, the form factor n also affects the magnetization's precession dynamics of the ellipsoidal nanoparticle.

3. Specifics of precession dynamics

Numerical solution of the equations (3) has been carried out using the Runge–Kutta method for the permalloy nanoparticle with the above material parameters. The parameters of the static field have been selected to be close to the resonance values at specified conditions of bias and pumping. Time dependence of the high-frequency field is specified as $\mathbf{h}(t) = \mathbf{h}_0 \sin\omega t$, where the amplitude $h_0 \ll H$, and the orientation $\mathbf{h}_0 \perp \mathbf{H}$.

The Fig. 3 shows the dependences of the resonance amplitude of the transverse high-frequency component M_x on the factor n, as obtained for the field $H = (50,\ 100,\ 150)$ Oe (the curves *1–3*) at the high-frequency field amplitude $h_0 = (0.1,\ 0.5)$ Oe (the thin and thick curves). The insert shows the dependence of the resonance frequency on the form factor n for the above values of the field H. It is clear that the precession amplitude dependence on the form factor is characterized by a maximum, which value depends both on the bias field, and on the high-frequency field: if with increase in H the maximum value decreases, then with increase in h_0 the value M_{xm} increases. The maximum is positioned by a value of the parameter n, at which the effective anisotropy field H_{KN} becomes zero.

Under bias of the ellipsoid of revolution along the symmetry axis and transverse pumping by the weak field ($h_0 \ll H$), one should expect relatively small precession amplitudes $M_{xm} \ll M_0$ and circular steady-state paths in the plane $(M_x,\ M_y)$ due to symmetry of precession and initial conditions $\varphi_0 = \theta_0 = 0$. Nevertheless, the Fig. 4 set of steady-state resonance paths corresponding to $H = 50$ Oe, $h_0 = 0.5$ Oe and the parameter values $n = 1.05,\ 1.00,\ 0.95,\ 0.94,\ 0.935,\ 0.93$ (the curves *1–6*) comprises not only circular, but elliptical paths as well. For n, at which $H_{\text{KN}} > 0$, all the paths are circular, whereas for n, at which $H_{\text{KN}} < 0$, the precession paths are undergoing more and more noticeable elliptical distortions with

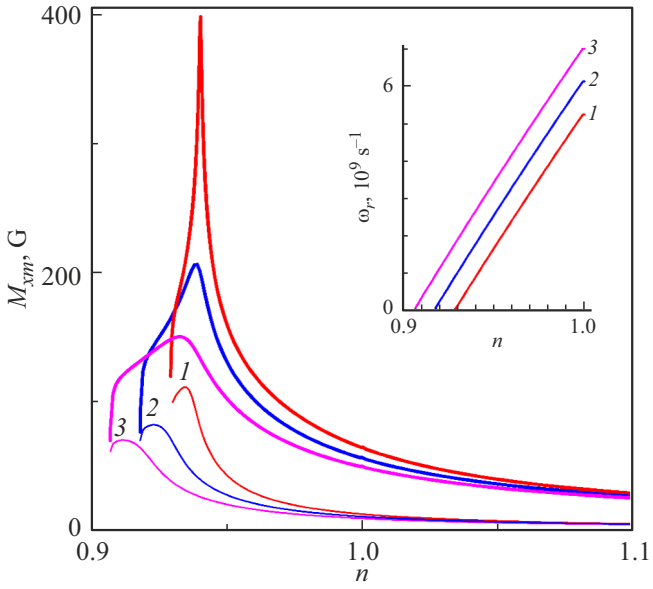

Figure 3. Dependences of the resonance amplitude of precession and the resonance frequency (on the insert) on the form factor, $H = 50,\ 100,\ 150$ Oe (the curves *1–3*), $h_0 = (0.1,\ 0.5)$ Oe (the thin and thick curves).

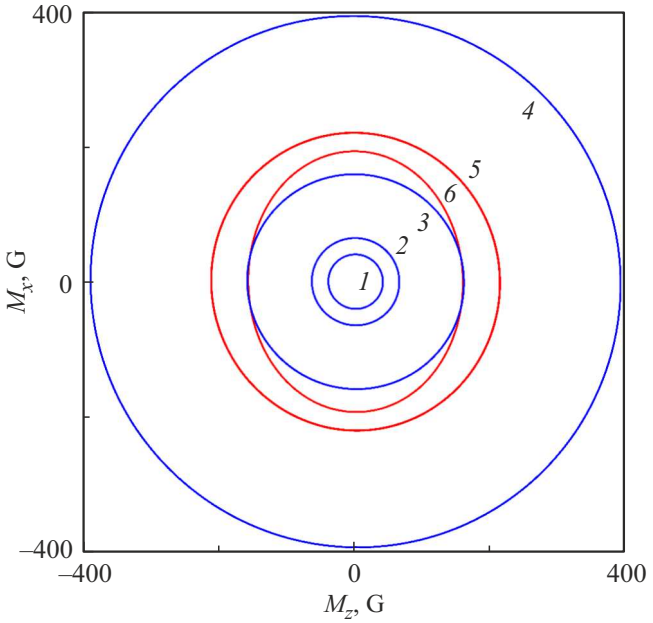

Figure 4. Resonance paths under NP bias along the „easy“ axis, which is parallel to the symmetry axis, $H = 50$ Oe, $h_0 = 0.5$ Oe, $n = 1.05$, 1.0, 0.95, 0.94, 0.935, 0.93 ($1-6$).

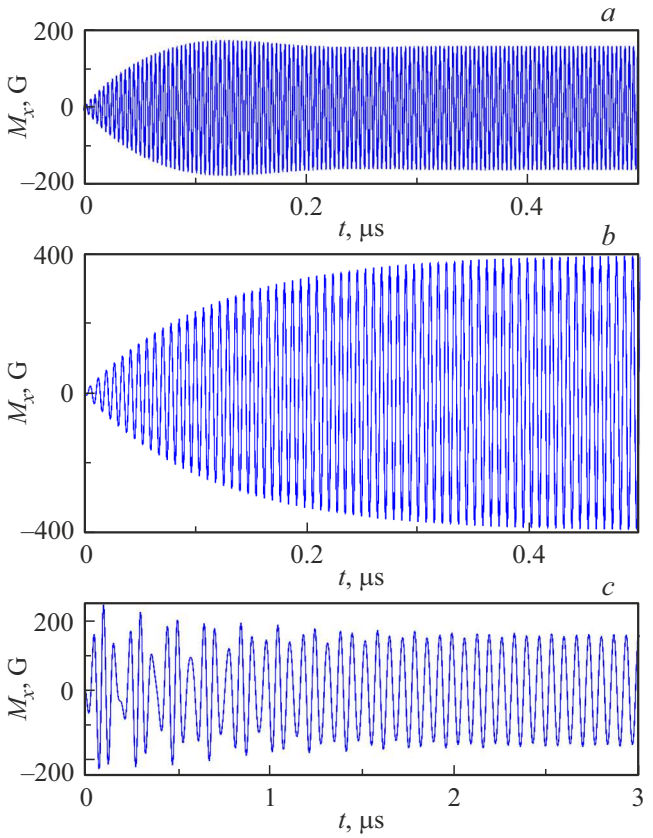

Figure 5. Time dependence of the x-component of magnetization when steady-state oscillations are becoming sustained, $n = 0.95$, 0.94, 0.93 ($a-c$), $H = 50$ Oe and $h_0 = 0.5$ Oe.

decrease in n. In these conditions, a nonlinear effect begins to appear distinctly, which consists in imposition of double frequency's nutation motion upon the circular precession of a high-frequency field frequency, thereby resulting in the path becoming elliptical. Attention is paid to the fact that with decrease in n the precession amplitude increases and at the value $n = 0.94$, to which $H_{\mathrm{KN}} = 0$ corresponds, the amplitude reaches the value $M_x = M_0/2$.

The Fig. 5, $a-c$ shows the dependence of the x-component of magnetization on time, when the steady-state oscillations are becoming sustained from an initial equilibrium state, for three cases corresponding to the paths *3, 4, 6* in the Fig. 4. It is clear that when getting onto the circular paths, a transient process is of a regular type (a, c). When getting to the elliptical path (at $n = 0.93$), the transient process is characterized by beats and the longest time interval (c) due to not only the least precession frequency, but to nonlinearity of the process as well.

Next, we will consider the frequency dependence of the magnetization amplitude of precession for the three cases discussed above $n < 1$ at $H = 50$ Oe and $h_0 = 0.5$ Oe. The Fig. 6 shows the frequency dependence of the maximum x-components of NP precession magnetization with $n = 0.95$, 0.94, 0.93 (the curves *1–3*). In the first two cases the precession oscillations are close to linear ones despite their large amplitude, and a value of the resonance frequency being implemented is close to the value to be determined using the formula (7). In case $n = 0.93$, the precession is substantially nonlinear and its maximum amplitude corresponds to the frequency $\omega \approx 2.7 \cdot 10^8\ \mathrm{s}^{-1}$, whereas the formula (7) yields the value $\omega_r \approx 1 \cdot 10^8\ \mathrm{s}^{-1}$.

Moreover, the latter case has an evident large frequency range, in which dynamic bistability is implemented, wherein under the same system parameters two steady-state precession modes with different characteristics can become sustained as affected by initial conditions and fluctuations. In this case the modes making up the bistability differ in terms of the precession amplitude by several times. In particular, the frequency $\omega \approx 2.5 \cdot 10^8\ \mathrm{s}^{-1}$ might have two steady-state precession modes implemented — with $M_{x\max} \approx 50$ G and with $M_{x\max} \approx 500$ G. Also, note that for the three presented cases the maximum precession amplitude is implemented at $n = 0.93$, which is attributed to a minimum effective field affecting the particle magnetization.

4. Conclusion

The analysis has been carried out to demonstrate that there is a number of evident nonlinearity-correlated features within the FMR spectrum of the single-domain ellipsoidal nanoparticle with the „easy“ axis coinciding with the symmetry axis under bias along this axis and conventional transverse pumping by the weak alternating field ($h_0 \ll H$). First of all, these include large resonance precession angles,

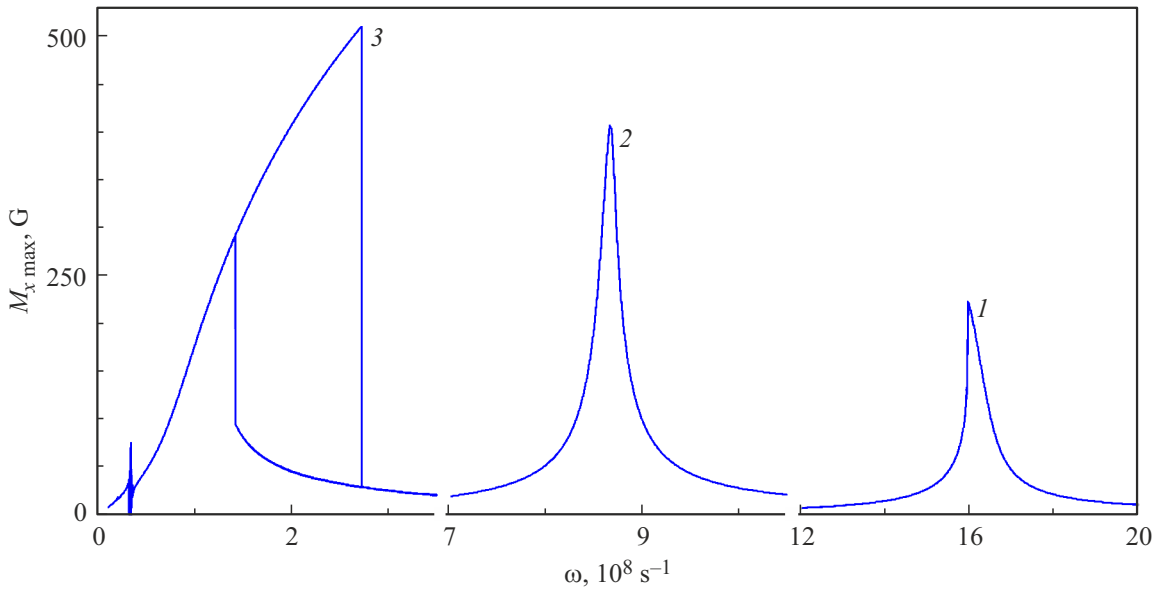

Figure 6. Frequency dependence of the resonance amplitude of precession, $n = 0.95,\ 0.94,\ 0.93$ (the curves *1–3*), $H = 50$ Oe, $h_0 = 0.5$ Oe.

at which the amplitude is $0.5M_0$; elliptical disturbances of the steady-state precession path at a negative value of the effective anisotropy field; presence of the frequency range, in which the dynamic bistability is implemented at $n = 0.93$ and the precession becomes substantially nonlinear.

Note that with the amplitude and frequency of the pumping field used in this paper, the homogeneous mode is largely removed in terms of the frequency from the spin-wave mode. That is why there is no energy transfer from the homogeneous precession to the spin waves and no development of spin-wave instabilities [22–24].

In the conclusion, we also indicate limitations being imposed on an NP size, which are correlated to a requirement of homogeneous magnetization [25]: the presence of the high-frequency field requires that the maximum NP size d was much smaller than a depth of a skin-layer δ. For the permalloy nanoparticle the condition $d \ll \delta \approx 10^{-4}$ cm must be met; thermal fluctuations may substantially affect the nanoparticle magnetization's precession dynamics. Their influence is described by a multiplier $\exp(-\Delta U/k_B T)$ [3], where ΔU — a potential barrier separating an „easy" and „hard" direction. Thermal excitation does not disturb the precession dynamics, if the NP size $d > d_{\min} \approx 10$ nm; an NP single-domain requirement to be met provided its radius is below $R_{cr} \approx \sigma_s/M_0^2$, where the surface energy of the domain boundary (for the permalloy $\sigma_s \approx 1$ erg/cm^2). That is why for the nanoparticle being investigated by us it is required that $d < 2R_{cr} \approx 30$ nm.

Thus, the most optimal NP size for FMR observation is $d \in (10-30)$ nm. However, note that according to data from the paper [26] metal particles with $d \approx (40-50)$ nm should be considered as single-domain ones.

Funding

This study was supported by Ministry of Science and Higher Education of the Russian Federation within the framework of the state assignment No. 0830-2020-0009.

Conflict of interest

The authors declare that they have no conflict of interest.

References

[1] E.Z. Meilikhov, R.M. Farzetdinova. JMMM **268**, 237 (2004).
[2] N. Eibagi, J.J. Kan, F.E. Spada, E.E. Fullerton. IEEE Magn. Lett. **3**, 4500204 (2012).
[3] E.Z. Meilikhov, R.M. Farzetdinova. Physics of the Solid State **56**, 2326 (2014).
[4] R. Berger, J.-C. Bissey, J. Kliava, H. Daubric, C. Estournéset. JMMM **234**, 535 (2001).
[5] R.B. Morgunov, A.I. Dmitriyev, G.I. Dzhardimaliyeva, A.D. Pomogaylo, A.S. Rosenberg, Y. Tanimoto, M. Leonowicz, E. Sowka. Physics of the Solid State **49**, *8*, 1436 (2007).
[6] G. Gubbiotti, G. Carlotty, T. Okuno, L. Giovannini, F. Montoncello, F. Nizzoli. Phys. Rev. B **72**, 184419 (2005).
[7] K.D. Usadel. Phys. Rev. B **73**, 212905 (2006).
[8] V.V. Kruglyak, S.O. Demokritov, D. Grundler. J. Phys. D **43**, 264001 (2010).
[9] A. Moser, K. Takano, D.T. Margulies, M. Albrecht, Y. Sonobe, Y. Ikeda, S.H. Sun, E.E. Fullerton. J. Phys. D **35**, *19*, R157 (2002).
[10] V. Flovik, F. Macia, J.M. Hernandez, R. Bručas, M. Hanson, E. Wahlström. Phys. Rev. B **92**, 104406 (2015).
[11] A.M. Biller, O.V. Stolbov, Yu.L. Raicher. Computational Continuum Mechanics **8**, *3*, 273 (2015).
[12] M.P. Wismayer, B.W. Southern, X.L. Fan, Y.S. Gui, C.-M. Hu, R.E. Camley. Phys. Rev. B **85**, 064411 (2012).

[13] M. Pardavi-Horvath, B.J. Ng, F.I. Gastano, H.S. Körner, C. Garcia, C.A. Ross. J. Appl. Phys. **110**, 053921 (2011).
[14] N.Yu. Grigoryeva, D.A. Popov, B.A. Kalinikos. Phys. Solid State **56**, *9*, 1806. (2014).
[15] A.M. Shutyi, D.I. Sementsov. Pis'ma v ZhETF **99**, *12*, 806 (2014) (in Russian).
[16] C. Wen-Bing, H. Man-Gui, Z. Hao, O. Yu, D. Long-Jiang. Chin. Phys. B **19**, *8*, 087502 (2010).
[17] E.V. Skorohodov, R.V. Gorev, R.R. Ykubov, E.S. Demidov, Yu.V. Khivintsev, Y. Filimonov, V.L. Mironov. JMMM **424**, 118 (2017).
[18] A.M. Shutyĭ, S.V. Eliseeva, D.I. Sementsov. Phys. Rev. B **91**, *2*, 024421 (2015).
[19] A.M. Shutyĭ, D.I. Sementsov. JMMM **401**, *3*, 1033 (2016).
[20] T.M. Vasilevskaya, A.M. Shutyi, D.I. Sementsov. Physics of the Solid State **64**, *2*, 200 (2022).
[21] A.G. Gurevich, G.A. Melkov. Magnetic oscillations and waves. Nauka, M. (1994).
[22] V.G. Shavrov, V.I. Shcheglov. Magnetization dynamics in conditions of its orientation change. Fizmatlit, M. (2019).
[23] M.A. Shamsutdinov, L.A. Kalyakin, A.T. Kharisov. Journal of Technical Physics **80**, *6*, 106 (2010).
[24] P.E. Zil'berman, A.G. Temiryazev, M.P. Tikhomirova. ZhETF **108**, 281 (1995) (in Russian).
[25] L.D. Landau, E.M. Lifshitz. Theoretical physics. Nauka, M. (1982). V. VIII.
[26] S.A. Nepiyko. Physical properties of small metal particles. Nauk. dumka, Kiev (1985).